



# Identification of a novel glycan processing enzyme with *exo*-acting $\beta$ -glucosidase activity in the Golgi apparatus using a new platform for the synthesis of fluorescent substrates



Wataru Hakamata<sup>\*</sup>, Kazuki Miura, Takako Hirano, Toshiyuki Nishio

Department of Chemistry and Life Science, College of Bioresource Sciences, Nihon University, 1866 Kameino, Fujisawa-shi, Kanagawa 252-0880, Japan

## ARTICLE INFO

### Article history:

Received 22 September 2014

Revised 13 November 2014

Accepted 14 November 2014

Available online 22 November 2014

### Keywords:

$\beta$ -Glucosidase

Golgi apparatus

Fluorescent substrate

Protein glycosylation

Glycan processing

Post-translational modification

Quinone methide cleavage

## ABSTRACT

The majority of eukaryotic proteins undergo post-translational modifications (PTMs) involving the attachment of complex glycans, predominantly through *N*-glycosylation and *O*-glycosylation. PTMs play important roles in virtually all cellular processes, and aberrant regulation of protein glycosylation and glycan processing has been implicated in various diseases. However, glycan processing on proteins in various cellular contexts has not been visualized. We had previously developed a quinone methide cleavage (QMC) platform for enhanced substrate design. This platform was applied here to screen for novel glycan-processing enzymes. We designed and synthesized fluorescent substrates with  $\beta$ -allopyranoside residues using the QMC platform. When applied in cell-based assays, the fluorescent substrates allowed rapid and clear visualization of  $\beta$ -glucosidase activity in the Golgi apparatus of human cultured cells. The QMC platform will likely find broad applications in visualizing the activities of glycan processing enzymes in living cells and in studying PTMs.

© 2014 Elsevier Ltd. All rights reserved.

## 1. Introduction

Although more than 300 post-translational modifications (PTMs) have been reported, many of these have only been described in eukaryotes.<sup>1</sup> PTMs comprise an array of reversible modifications that promote signaling diversity and the rapid conveyance of cellular messages.<sup>2</sup> Some irreversible PTMs, including glycosylation, lipidation, and disulfide bond formation, are stable and are important for the maturation and proper folding of nascent proteins.<sup>3</sup> Protein glycosylation involves the attachment of monosaccharides and glycans to proteins and provides greater proteomic diversity than do other PTMs.<sup>4</sup> Protein glycosylation is mediated by various glycosyltransferases such as oligosaccharyl-transferase (OST, EC 2.4.1.119) and is processed by an *exo*-acting glycan-processing enzyme such as endoplasmic reticulum (ER) glucosidase I and II, resulting in the attachment of various *N*- and *O*-linked glycans. The majority of secretory proteins are

co-translationally appended with asparagine-linked oligosaccharides (*N*-glycans). *N*-glycans and *N*-glycan processing enzymes are thought to play important roles in protein quality control during protein synthesis and folding, functions that are essential for cellular health.<sup>5</sup> In contrast, the hydroxyl groups of serine and threonine in various proteins are labeled with *O*-linked oligosaccharides (*O*-glycans). *O*-Glycans and *O*-glycan processing enzymes are thought to play important roles not only in protection of mucosa but also in abnormal behavior at the cellular level and the avoidance of immunological defenses by cancer cells. These functions are essential for the proliferation of cancer cells.<sup>6</sup> Despite their importance in maintaining cellular health and promoting cancerous growths, the development of technology for visualizing most glycan-processing enzyme activities remains an important challenge. Several fluorescent substrates are commercially available for visualizing and monitoring  $\alpha$ -mannosidase and  $\beta$ -galactosidase as *exo* glycan intracellular hydrolase activity in cultured cells (Fig. 1). In the future, these substrates may facilitate functional imaging analysis of protein glycosylation. Previous molecular designs of glycan-processing enzyme substrates have not targeted active sites using 3-dimensional enzyme structures. In general, the active sites of *exo*-acting glycan-processing enzymes are composed of subsite  $-1$ , which recognizes a sugar moiety at the non-reducing end of the substrate, and subsite  $+1$ , which

Abbreviations: 2MeTG, 2-methyl TokyoGreen; BFA, brefeldin A; EM, emission wavelength; ER, endoplasmic reticulum; EX, excitation wavelength; Man, mannose; MS, mass spectrometry; NMR, nuclear magnetic resonance; PBS, phosphate-buffered saline; PTM, post-translational modifications; QMC, quinone methide cleavage; TBP, tributyl phosphine; TFMU, 4-Trifluoromethylumbelliferone.

<sup>\*</sup> Corresponding author.

E-mail address: [hakamata.wataru@nihon-u.ac.jp](mailto:hakamata.wataru@nihon-u.ac.jp) (W. Hakamata).

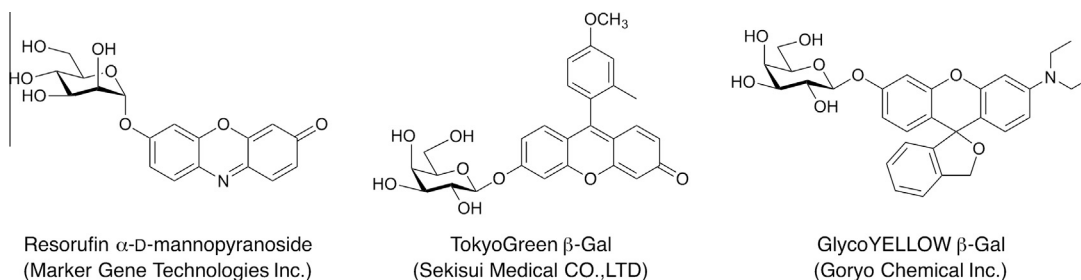


**Figure 1.** Structure of commercially available fluorescent substrates for  $\alpha$ -mannosidase and  $\beta$ -galactosidase in cultured cells.

recognizes the penultimate sugar moiety at the non-reducing end. Hydrolysis occurs between subsites  $-1$  and  $+1$ .<sup>7–9</sup> Using small synthetic molecules to design the substrate, we previously reported the molecular recognition of an active site in ER glucosidases functioning as *N*-glycan processing enzymes.<sup>10,11</sup> To develop practical substrates that are operational in cells, it is essential to base the precise molecular design of substrates on known structural information for glycan-processing enzymes.

Commercially available fluorescent substrates targeting the modeled enzyme subsites bind subsite  $+1$  poorly, which may be due to steric hindrance and a flat, non-sugar-like structure on the part of the fluorophore. Reducing the size of fluorophores is impractical because small-sized fluorescent moieties have low quantum yields, decreasing their sensitivity. Therefore, a different substrate-design platform is required to design fluorescent substrates for *exo* glycan-processing enzymes. Our group reported the development of a substrate-design platform using quinone methide cleavage (QMC) reactions to study the activity of an ER-localized endogenous carboxyl esterase as a pro-drug activation enzyme. The multicolor fluorescence probes detected carboxyl esterases in the ER via two-step reactions: ester hydrolysis and spontaneous QMC reaction at the cellular level. These probes penetrate into the ERs, after hydrolysis, the release and accumulation of water insoluble fluorophores from these probes specifically stained ERs with bright fluorescence in 3 human cell lines.<sup>12,13</sup> To develop probes with improved binding to subsite  $+1$  of the enzyme active site, we applied the QMC platform for substrate design of an *exo* glycan-processing enzyme involved in *N*- and *O*-glycan processing (Fig. 2). The sugar and benzyl moieties of the substrates occupy subsite  $-1$  and subsite  $+1$ , respectively. The substrate fluorophore is located outside of the enzyme active site. A schematic representation of our designed substrates and commercially available substrates bound to enzyme subsites is shown in Figure 3A and 3B, respectively.

The present study describes a new imaging technology for identifying glycan-processing enzymes using fluorescently labeled substrates, based on the QMC platform. These substrates can also be used to conduct mechanistic experiments in living cells by confocal microscopy. Thus, our platform may also reveal novel glycan-processing enzymes in living cells. To demonstrate the potential of

our QMC platform in discovering novel glycan-processing enzymes, we sought to identify *exo*-acting  $\beta$ -allosidase activity as an undiscovered activity in human cells. Allose, which is an epimer of glucose at the C-3 hydroxyl group, is a rare sugar. Yanagita et al. reported the anti-proliferative activity of 6-*O*-acetyl-D-allose against the human leukemia MOLT-4F cell line.<sup>14</sup> If  $\beta$ -allosidase activity is observed in human cells, we can postulate the existence of  $\beta$ -allosidase as an important player of an undiscovered physiological function. Moreover,  $\beta$ -allosidases potentially regulate novel pathways of *N*- and *O*-glycan processing and may serve as novel targets for drug discovery. We report herein the design and synthesis of a QMC platform based on novel fluorescent substrates for measuring  $\beta$ -allosidase activity in human cultured cells. Using these substrates, we also localized the  $\beta$ -allosidase activity to the Golgi apparatus in human cultured cells with bright fluorescence.

## 2. Material and methods

### 2.1. Substrate synthesis

Structures of all designed substrates **1–6** are shown in Figure 5. The fluorescent substrates **1–3** and **6** were synthesized to evaluate  $\beta$ -allosidase activities in living cells. Details of the synthetic scheme of **1–3** and **6** are outlined in Figure S1. The starting material (4-formylphenyl  $\beta$ -D-allopyranoside) of **1–3** and **6** was acetylated,<sup>15</sup> and an aldehyde of obtained acetyl derivative was reduced to a benzyl alcohol derivative using NaBH<sub>4</sub>. In the next step, Mitsunobu reaction conditions<sup>12,13</sup> were used to react the benzyl alcohol derivative with the fluorophores resorufin, TFMU, or 2MeTG,<sup>16,17</sup> yielding substrates **1–3**, respectively. Substrate **4** was synthesized by deacetylation of compound **3**. The materials used for substrate synthesis, the synthesis details, and the instrumental analysis of substrates **1–3** and **6** are described in the Supplementary data.

### 2.2. Cell-based assays

Cell-base assays for measuring  $\beta$ -allosidase activity were performed using substrates **1–3**, substrate **6**, and Golgi-ID Green with HT-1080, HeLa, and SK-N-SH cells. Co-staining assays with

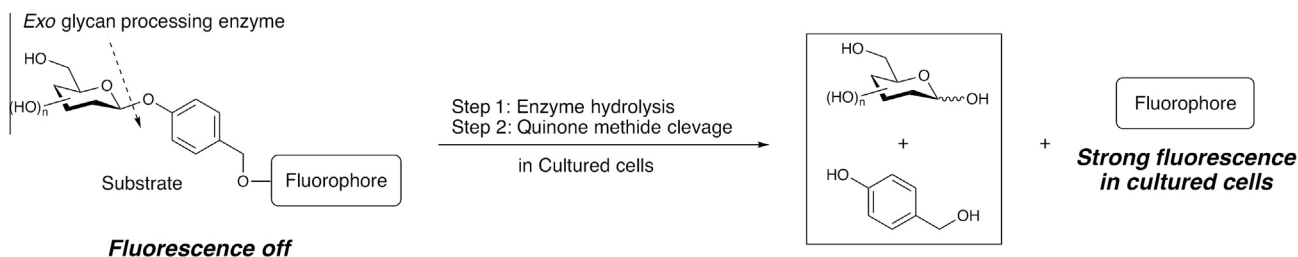


**Figure 2.** Rational design of substrates for an *exo* glycan-processing enzyme, based on the QMC platform.

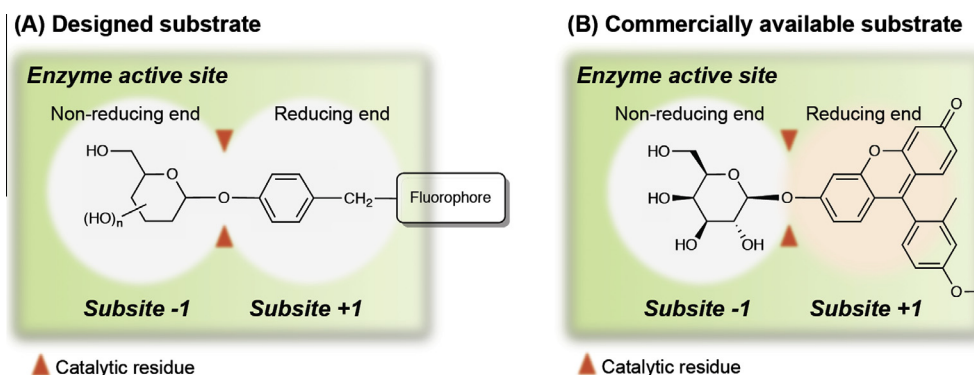


**Figure 3.** Schematic diagrams of subsite structures of an *exo* glycan-processing enzyme. (A) QMC-based designed substrate bound in the active site. (B) Poor fitting of a commercially available substrate in subsite +1.

substrate **1** and Golgi-ID Green were also performed with each of the 3 cell lines. We further determined the identity of the stained organelle in HT-1080 cells using by substrate **6** and BFA. All fluorescence signals in cells were recorded using a confocal laser-scanning microscope. The materials and methods used for performing cell-based assays are described in the [Supporting information](#).

### 3. Results and discussion

#### 3.1. Design and synthesis of fluorescent $\beta$ -glucosidase substrates based on the QMC platform

To confirm the efficacy of adapting our QMC platform-based substrates for targeting enzyme active sites, we performed a molecular docking study to analyze the interactions of 3 ligands with human class I  $\alpha$ -1,2-mannosidase (PDB ID: 1X9D), an *exo*-acting, *N*-linked glycan-processing enzyme.<sup>18</sup> For this computational study, we analyzed 3 substrates: a natural substrate (Man  $\alpha$ -1,2 Man), a QMC platform-based mannosidase substrate with 2MeTG, and a commercially available mannosidase substrate. Our docking models demonstrated potential interactions between each substrate and the enzyme subsites. The Man  $\alpha$ -1,2 Man moiety of the non-reducing end of the natural substrate was predicted to occupy subsites -1 and +1 of the enzyme active site. The Man residue of reducing end of the substrate was exposed to the solvent

surface, as shown in [Figure 4A](#). The  $\alpha$ -mannopyranoside and benzyl moieties of the QMC-based substrate occupied subsites -1 and +1, respectively. The 2MeTG fluorophore of the QMC-based substrate was located outside of the enzyme active site, as shown in [Figure 4B](#). The commercially available substrate was not predicted to occupy subsite -1. The  $\alpha$ -mannopyranoside moiety of the commercially available substrate occupied subsite +1 and the 2MeTG fluorophore of the substrate was located outside of enzyme active site, as shown in [Figure 4C](#). Given these results, QMC platform-based substrates for  $\beta$ -glucosidase are predicted to have greater compatibility with subsite +1 of the enzyme than are commercially available substrates and some reported substrates.<sup>19,20</sup>

We designed 6 fluorescent  $\beta$ -glucosidase substrates based on the QMC platform and docking study of human class I  $\alpha$ -1,2-mannosidase as it provides suitable models for enzyme–ligand complex, as shown in [Figure 5](#). Cleavage of these substrates by  $\beta$ -glucosidase in cultured cells can occur through 2 reactions, namely  $\beta$ -alloypyranoside linkage hydrolysis and QMC reactions. Hydrolysis releases the fluorophore from the substrate, staining the organelle that the  $\beta$ -glucosidase enzyme resides in.  $\beta$ -Glucosidase substrates **1–6** showed the following EX and EM maxima: resorufin (EX, 571 nm; EM, 585 nm), TFMU (EX, 385 nm; EM, 502 nm), and 2MeTG (EX, 491 nm; EM, 510 nm),<sup>12,13</sup> producing red, blue, and green fluorescence, respectively. These fluorophores also show distinct EX and EM, excellent fluorescence quantum yields, and low pH-dependent

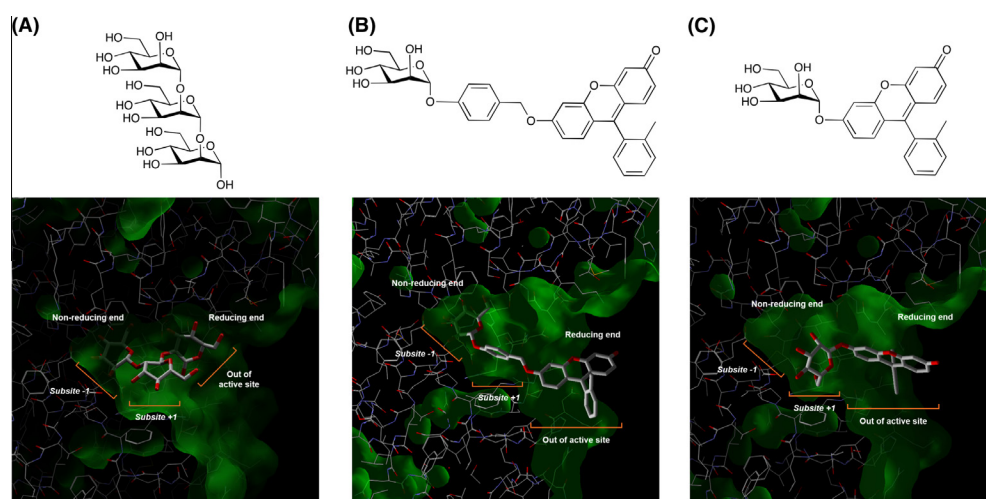


**Figure 4.** Molecular modeling of the lowest-energy complex of human Golgi mannosidase bound with a mannopyranoside derivative. (A) Magnified view of the enzyme-natural substrate complex. (B) Magnified view of the enzyme-QMC platform-based substrate complex. (C) Magnified view of the enzyme-commercially available substrate complex.

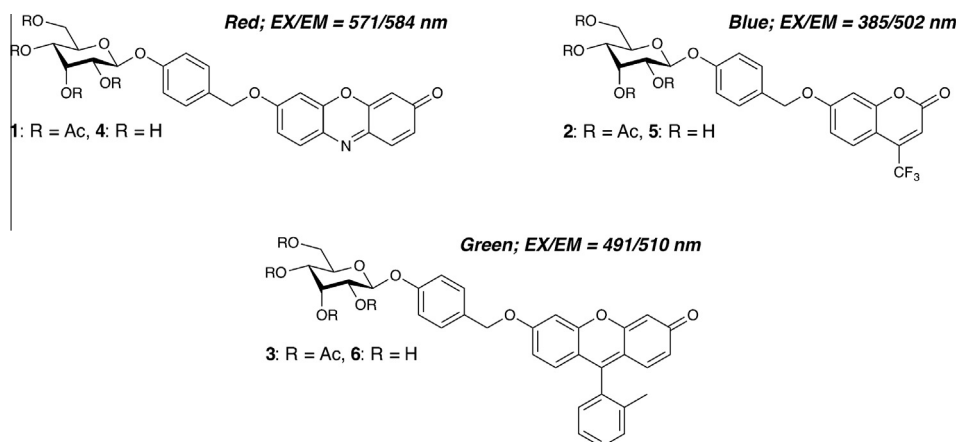


**Figure 5.** Structure of QMC platform-based substrates for  $\beta$ -allosidase.

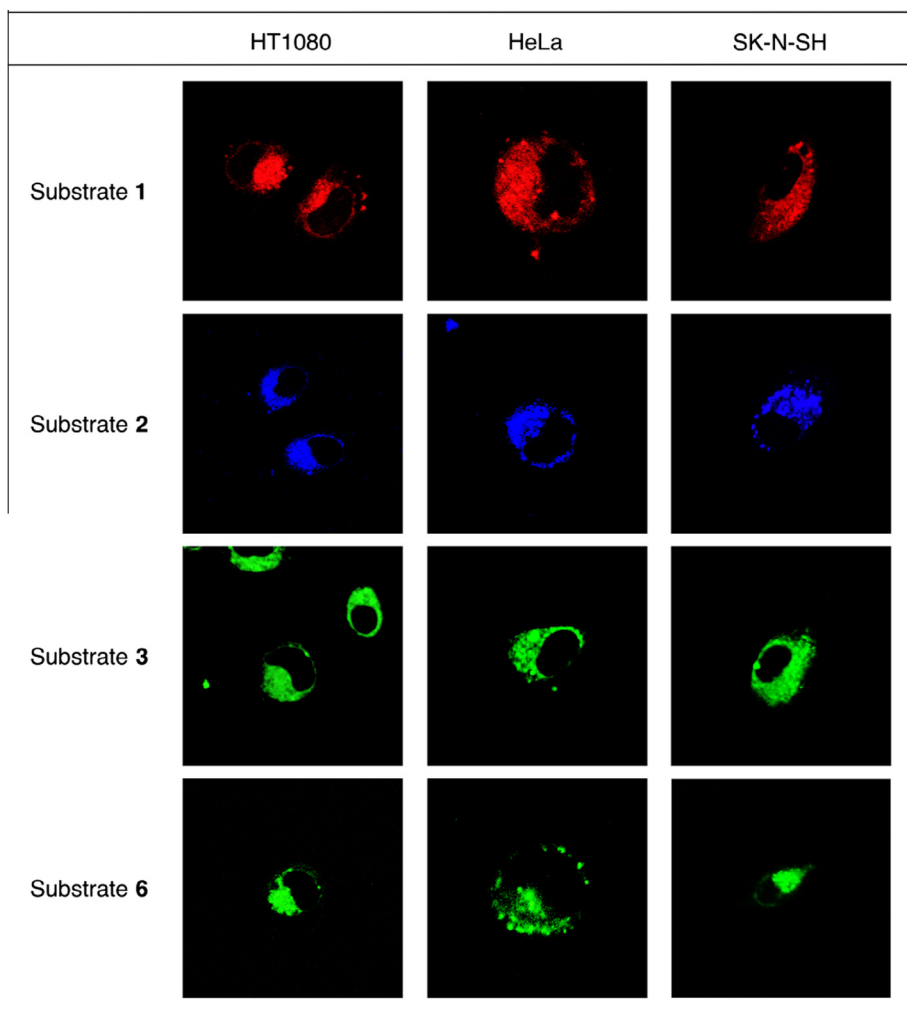


**Figure 6.** Fluorescence images of three different cell lines showing the location of substrate hydrolysis. Substrates **1–3** and **6**, each tagged with a specific color fluorophore, were introduced to three cell types, HT1080, HeLa, and Sk-N-SH. Substrate **1** was tagged with resorufin (red), while substrate **2** was tagged with TFMU (blue). Substrates **3** and **6** were both tagged with 2MeTG (green).

changes in fluorescence, which make them suitable for multicolor imaging of enzyme activity in living cells. Thus, these fluorophores and related derivatives are used widely in biological research. Moreover, these designed substrates exhibit membrane permeability, making them compatible for use as fluorescent bioimaging

tools. Results from a previous study with Caco-2 cells showed that a  $\log D$  value of  $>4.5$  is required for compounds with molecular weights  $>500$  to have high membrane permeability.<sup>21</sup> The  $\text{clog}D$  values of substrates **1–6** were calculated,<sup>22</sup> and the resulting values were evaluated based on above index. Substrates **4** and **5** lack

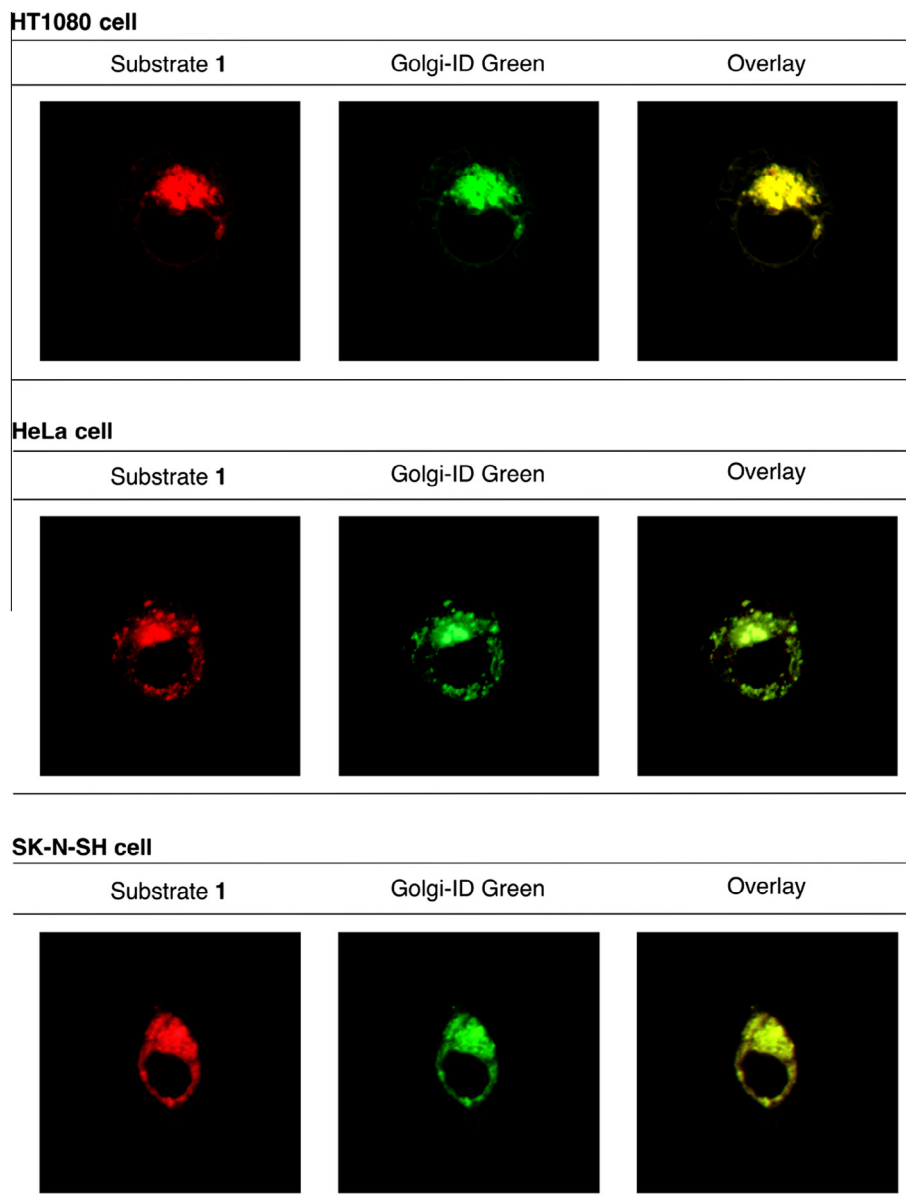


**Figure 7.** Fluorescence images of substrate **1** (resorufin; red) and Golgi-ID Green (green) expression, as well as the merged fluorescence images, indicating the co-localization of the substrate and the Golgi apparatus-specific dye in three cell lines.

acetyl groups and showed low *clogD* values (data not shown). In contrast, substrates **1–3** and **6**, which have molecular weights of 650, 612, 738, and 571 had *cLogD* values of 4.20, 3.36, 7.43, and 4.73, respectively, at physiological pH in cells, indicative of adequate membrane permeability. An acetyl modification of substrate hydroxyl groups to improve membrane permeability may raise concerns regarding deacetylation in cells living. However, numerous commercially available bioimaging probes have acetyl groups that are hydrolyzed and activated by cytosolic esterases.<sup>23</sup>

Considering these results, substrates **1–3** and **6** were synthesized in preparation for testing in cell-based assays. To be useful as  $\beta$ -glucosidase substrates and multicolor bioimaging tool in cells, the fluorescence from substrates **1–3** and **6** should show minimal emission before hydrolyzation, as was observed with substrates **1–3** and **6** in PBS. Therefore, these substrates will be in a quenched state in cells before hydrolyzation. For synthesis details, <sup>1</sup>H NMR, <sup>13</sup>C NMR, MS, elemental analysis (C, H, N, and F), and fluorescence spectra of substrates **1–3** and **6**, refer to the METHODS and Supporting information sections.

### 3.2. Fluorescence of QMC platform-based substrates in cultured human cells

To screen for  $\beta$ -glucosidase activity in cultured cells, we incubated a human fibrosarcoma cell line (HT-1080), a human cervical cancer cell line (HeLa), and a human neuroblastoma cell line (SK-N-SH) with substrates **1–3** and **6**, at final concentrations of 10  $\mu$ M. The resulting fluorescence signals were imaged using a confocal laser-scanning microscope. Fluorescence signaling from substrates **1–3** (with acetyl groups) and substrate **6** (without an acetyl group) revealed an intracellular accumulation of each fluorophore in the nuclear peripheries (Fig. 6), suggesting that they were cleaved both by  $\beta$ -glucosidase and esterase enzymes. The fluorescence intensities of substrates **1–3** and **6** generated by  $\beta$ -glucosidase activity in each cell line was independent of fluorophore structures and acetyl modification. The substrates bound to subsite –1 and subsite +1 of  $\beta$ -glucosidase, and the enzyme has no recognition site for the fluorophore based on molecular modeling data with a mannosidase. Moreover, substrates **1–3** and **6** stained the



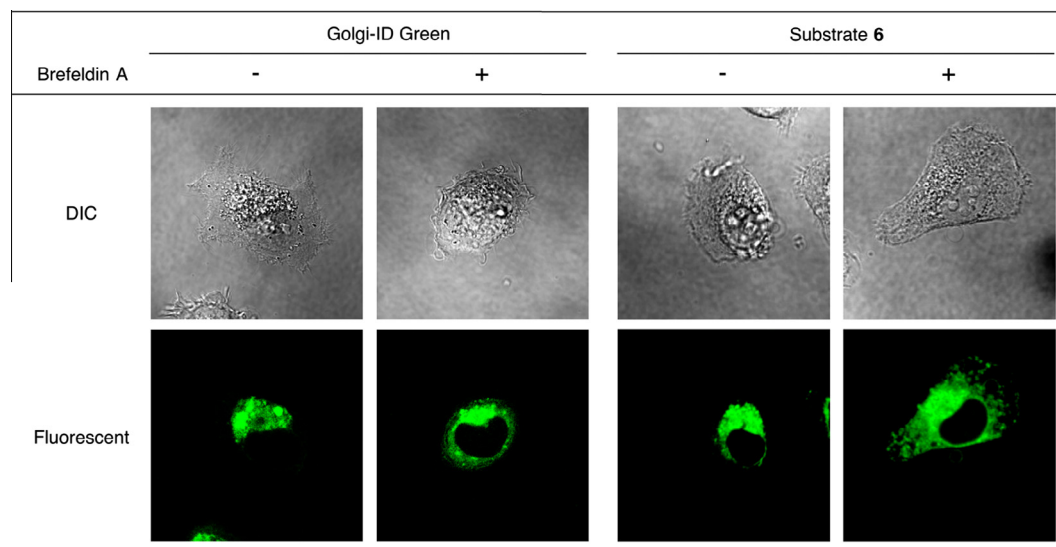


**Figure 8.** Fluorescence images of HT-1080 cells stained with Golgi-ID Green and Substrate **6** (both green) following dispersion of the Golgi apparatus with BFA along with differential interference contrast microscopy (DIC) images highlighting the altered morphology of the cells.

same cellular compartment. A dynamic equilibrium may occur as deacetylated substrates are transferred into the lumens of organelles and are then trapped by hydrolysis at the  $\beta$ -allopyranoside linkage. The pattern of bright fluorescence observed around the nuclear peripheries suggested that the fluorescent substrates were localized to the Golgi apparatus, as a reticulated staining pattern characteristic of the ER was not observed.

### 3.3. $\beta$ -Allosidase activity in the Golgi apparatus

The subcellular localization of the observed  $\beta$ -allosidase activity was investigated using a commercially available organelle-specific dye. A well-known fluorescent reagent for the Golgi apparatus, Golgi-ID Green (EX, 473 nm; EM, 543 nm), was used to co-stain HT-1080, HeLa, and SK-N-SH cells with substrate **1**. Substrate **1** contains resorufin as the fluorophore, which provides a fluorescence window that is distinct from Golgi-ID Green. The capacity for generating alternative fluorescence wavelengths by the QMC platform allows flexibility in selecting the most suitable substrates for biological observations. Fluorescence signaling in cells co-stained with substrate **1** and Golgi-ID Green was evident in all 3 cell lines. Moreover, substrate **1** and Golgi-ID Green fluorescence colocalized to the Golgi apparatus, as shown in Figure 7. It is evident from these observations that substrates **1–3** and **6** were specifically hydrolyzed in the Golgi apparatus. In parallel experiments, we analyzed the dispersion of the stained Golgi apparatus caused by BFA. BFA inhibits the transport of proteins from the ER to the Golgi apparatus; consequently, the Golgi apparatus is dispersed in living cells.<sup>24</sup> Treatment of HT-1080 cells with BFA and either Golgi-ID Green or substrate **6** revealed similar morphological and staining patterns in the Golgi apparatus, as shown in Figure 8. In these cell-based assays, traces of released fluorophore leaking out of the Golgi apparatus were observed. After carefully considering the concern, it is evident from our data that the Golgi apparatus of human cells possesses  $\beta$ -allosidase.

## 4. Conclusion

We successfully developed a QMC platform for synthesizing fluorescent substrates of *exo* glycan-processing enzymes, based on the known subsite structures. Fluorescent substrates **1–3** and

**6** can be used to investigate the role of  $\beta$ -allosidase in glycan processing and to determine aberrant activities in diseases. The preliminary conclusions were reached that the Golgi apparatus of human cells contains active  $\beta$ -allosidase. Further consideration will be needed to yield any findings about an isolation of  $\beta$ -allosidase and a determination of enzymatic properties. Substrates **1–3** and **6** also provide a starting point for developing fluorescent substrates to explore novel glycan-processing enzymes mediating PTMs in living cells. The results of this study provide a good example of the utility of the QMC platform for designing substrates of glycan-processing enzymes; thus, this platform should be useful for analyzing both static and dynamic events in biological applications. Using this strategy, we are currently building a library of fluorescent substrates for *exo* glycan-processing hydrolases involved in PTMs, such as glucosidase in the ER, mannosidase in the ER and Golgi apparatus, and fucosidase in the lysosome, which will greatly impact the bioimaging field of glycobiology. Glycosylation studies deeply affected our understanding of PTMs in the last century. Similarly, the bioimaging of processing enzyme activities in living cells should advance our understanding of protein glycosylation and provide breakthroughs needed to monitor glycan-processing pathways in live cells.

## Acknowledgments

The authors wish to express their sincere thanks to Mrs. T. Kiu-chi of the General Research Institute of the College of Bioresource Sciences of Nihon University for performing FAB/MS measurements and Mrs. A. Sato of A-Rabbit-Science Japan Co., Ltd for performing the elemental analyses. This work was partly supported by JSPS KAKENHI Grant Number 26460157.

## Supplementary data

Supplementary data associated with this article can be found, in the online version, at <http://dx.doi.org/10.1016/j.bmc.2014.11.023>.

## References and notes

- Witze, E. S.; Old, W. M.; Resing, K. A.; Ahn, N. G. *Nat. Methods* **2007**, *4*, 798.
- Deribe, Y. L.; Pawson, T.; Dikic, I. *Nat. Struct. Mol. Biol.* **2010**, *17*, 666.
- Siman, P.; Brik, A. *Org. Biomol. Chem.* **2012**, *10*, 5684.

4. Pan, S.; Chen, R.; Aebersold, R.; Brentnall, T. A. *Mol. Cell Proteomics* **2011**, 10, R110.003251.
5. Needham, P. G.; Brodsky, J. L. *Biochim. Biophys. Acta* **2013**, 1833, 2447.
6. Brooks, S. A.; Carter, T. M.; Royle, L.; Harvey, D. J.; Fry, S. A.; Kinch, C.; Dwek, R. A.; Rudd, P. M. *Anticancer Agents Med. Chem.* **2008**, 8, 2.
7. Kurakata, Y.; Uechi, A.; Yoshida, H.; Kamitori, S.; Sakano, Y.; Nishikawa, A.; Tonozuka, T. *J. Mol. Biol.* **2008**, 381, 116.
8. Karaveg, K.; Siriwardena, A.; Tempel, W.; Liu, Z. J.; Glushka, J.; Wang, B. C.; Moremen, K. W. *J. Biol. Chem.* **2005**, 280, 16197.
9. Shah, N.; Kuntz, D. A.; Rose, D. R. *Proc. Natl. Acad. Sci. U.S.A.* **2008**, 105, 9570.
10. Hakamata, W.; Muroi, M.; Nishio, T.; Oku, T.; Takatsuki, A. *J. Carbohydr. Chem.* **2004**, 23, 27.
11. Hakamata, W.; Kurihara, M.; Okuda, H.; Nishio, T.; Oku, T. *Curr. Top. Med. Chem.* **2009**, 9, 3.
12. Hakamata, W.; Machida, A.; Oku, T.; Nishio, T. *Bioorg. Med. Chem. Lett.* **2011**, 21, 3206.
13. Hakamata, W.; Tamura, S.; Hirano, T.; Nishio, T. *ACS Med. Chem. Lett.* **2014**, 5, 321.
14. Yanagita, R. C.; Kobashi, K.; Ogawa, C.; Ashida, Y.; Yamaashi, H.; Kawanami, Y. *Biosci. Biotech. Biochem.* **2014**, 78, 190.
15. Ye, D.; Zhang, K.; Chen, H.-F.; Yin, S.-F.; Li, Y. *Struct. Rep. Online* **2009**, 65, o1338.
16. Urano, Y.; Kamiya, M.; Kanda, K.; Ueno, T.; Hirose, K.; Nagano, T. *J. Am. Chem. Soc.* **2005**, 127, 4888.
17. Mottram, L. F.; Boonyarattanakalin, S.; Kovel, R. E.; Peterson, B. R. *Org. Lett.* **2006**, 8, 581.
18. CLC bio, a QIAGEN Company Inc, Molegro Virtual Docker Ver. 6.0.
19. Kamiya, M.; Asanuma, D.; Kuranaga, E.; Takeishi, A.; Sakabe, M.; Miura, M.; Nagano, T.; Urano, Y. *J. Am. Chem. Soc.* **2011**, 133, 12960.
20. Ichikawa, Y.; Kamiya, M.; Obata, F.; Miura, M.; Terai, T.; Komatsu, T.; Ueno, T.; Hanaoka, K.; Nagano, T.; Urano, Y. *Angew. Chem., Int. Ed.* **2014**, 53, 6772.
21. Waring, M. J. *Expert Opin. Drug Discovery* **2010**, 5, 235.
22. Advanced Chemistry Development Inc., Structure Design Suite Ver. 12.
23. Products list: Carboxy-H2DFFDA, C-13293, H2DCFDA, D-399, Oregon green carboxylic acid diacetate, O6151 (Molecular Probes); FluoForte Calcium Assay Kit, ENZ-51017, eFluxx-ID Green Multidrug Resistance Assay Kit, ENZ-51029 (ENZO Life Sciences); HaloTag diAcFAM Ligand, G8273, (Promega).
24. Fujiwara, T.; Oda, K.; Yokota, S.; Takatsuki, A.; Ikehara, Y. *J. Biol. Chem.* **1988**, 263, 18545.